

Individual differences in functional brain connectivity predict temporal discounting preference in the transition to adolescence



Jeya Anandakumar^{a,1}, Kathryn L. Mills^{b,*1}, Eric A. Earl^a, Lourdes Irwin^a, Oscar Miranda-Dominguez^a, Damion V. Demeter^e, Alexandra Walton-Weston^a, Sarah Karalunas^c, Joel Nigg^c, Damien A. Fair^{a,c,d}

^a Department of Behavioral Neuroscience, Oregon Health & Science University, Portland, OR, United States

^b Department of Psychology, University of Oregon, Eugene, OR 97403, United States

^c Department of Psychiatry, Oregon Health & Science University, Portland, OR, United States

^d Advanced Imaging Research Center, Oregon Health & Science University, Portland, OR, United States

^e Department of Psychology, University of Texas at Austin, Austin, TX, United States

ARTICLE INFO

Keywords:

Delay discounting

fMRI

Intrinsic connectivity

Longitudinal

Resting state

ABSTRACT

The transition from childhood to adolescence is marked by distinct changes in behavior, including how one values waiting for a large reward compared to receiving an immediate, yet smaller, reward. While previous research has emphasized the relationship between this preference and age, it is also proposed that this behavior is related to circuitry between valuation and cognitive control systems. In this study, we examined how age and intrinsic functional connectivity strength within and between these neural systems relate to changes in discounting behavior across the transition into adolescence. We used mixed-effects modeling and linear regression to assess the contributions of age and connectivity strength in predicting discounting behavior. First, we identified relevant connections in a longitudinal sample of 64 individuals who completed MRI scans and behavioral assessments 2–3 times across ages 7–15 years (137 scans). We then repeated the analysis in a separate, cross-sectional, sample of 84 individuals (7–13 years). Both samples showed an age-related increase in preference for waiting for larger rewards. Connectivity strength within and between valuation and cognitive control systems accounted for further variance not explained by age. These results suggest that individual differences in functional brain organization can account for behavioral changes typically associated with age.

1. Introduction

Temporal discounting (also known as inter-temporal choice or delay discounting) is the process of assessing the value of waiting for a future reward depending on the magnitude of the reward and the delayed time. Individuals vary in their temporal discounting behavior, with some having a stronger preference for taking a smaller immediate reward versus waiting for a larger reward, and vice versa (Sadaghiani and Kleinschmidt, 2013). Previous experimental studies suggest a positive relationship between chronological maturation (age) and the tendency to prefer waiting for the larger reward (de Water et al., 2014; Steinberg et al., 2009), although some studies have found evidence for a non-linear relationship in the transition into adolescence (Scheres et al., 2014). Interestingly, the development of temporal discounting with age may be a stable marker of liability for disinhibitory psychopathologies

such as ADHD even when psychopathological symptoms change with age (Karalunas et al., 2017). It has been proposed that brain function and organization can explain individual differences in temporal discounting behavior (Christakou et al., 2011; Hare et al., 2014; Li et al., 2013; Scheres et al., 2013; van den Bos et al., 2014). Therefore, in this study, we analyzed how chronological maturation interacts with functional brain organization to predict temporal discounting.

1.1. Temporal discounting as a measure of decision-making preference

Tasks assessing temporal discounting behavior can be used to measure an individual's preference for a smaller-sooner reward (SSR) in comparison to a larger-later reward (LLR) (Green et al., 1997). These tasks typically ask individuals to choose between two rewards that vary in both the reward size and the required delay time until the amount is

* Corresponding author.

E-mail address: klmills@uoregon.edu (K.L. Mills).

¹ Contributed equally to this work.

acquired (Myerson and Green, 1995). For example, participants typically respond to several questions in the following format: “At the moment, what would you prefer?” Below the question two options are presented (e.g. “\$7.00 now”, “\$10 in 30 days”). The SSR and LLR vary in both delay interval and reward size over successive trials; this way, the subjective value of temporal reward can be measured. Individuals preferring the SSR are characterized to have greater temporal discounting; conversely, individuals preferring the LLR are characterized to have less temporal discounting. One way to measure this subjective value of temporal reward is through the use of indifference points (the delay duration at which the magnitude of SSR equals the magnitude of LLR) (Richards et al., 1999). The indifference points are useful in calculating a single index of discounting rate, and in determining the value of the delayed reward (Yi et al., 2010). Specifically, plotting the indifference points in a series yields a discount curve, which describes the rate at which the value of reward decreases over time.

1.2. Brain networks involved in temporal discounting

Cortico-striatal circuitry is involved in decision-making processes (Haber and Knutson, 2009), including temporal discounting (Peters and Büchel, 2011). In the present study, we focus on two cortico-striatal systems (defined *a priori*) that have been consistently correlated with different outcomes of an individual's preference and value (Peters and Büchel, 2011; van den Bos et al., 2014): a valuation system (amygdala, medial orbitofrontal cortex, posterior cingulate cortex, ventromedial prefrontal cortex, and ventral striatum) and a cognitive control system (ventral lateral prefrontal cortex, dorsal anterior cingulate cortex, dorsolateral prefrontal cortex, dorsal striatum, and inferior frontal cortex) (See Fig. 1a). Specifically, increased structural connectivity between the striatum and cortical control regions have been found to be related to decreased temporal discounting, whereas increased structural connectivity between the striatum and subcortical valuation regions were related to increased temporal discounting in adults (van den Bos et al., 2014). We also assessed connectivity between these networks and the supplementary motor area and hippocampus, given their involvement in intertemporal choice behavior (Peters and Büchel, 2010; Scheres et al., 2013; van den Bos et al., 2014).

Brain networks involved in temporal discounting can be interrogated with MRI in multiple ways, including task-based fMRI studies in which participants are asked to make temporal discounting decisions. Overall, it has been theorized that adults with high temporal discounting preference are more likely to show greater recruitment of the control network and less recruitment of the valuation network when choosing a LLR over a SSR (van den Bos and McClure, 2013; Volkow and Baler, 2015). While task-evoked brain activity can inform us on the functionality of cortical networks during specific contexts, intrinsic brain activity at rest can be used to measure an individual's functional brain organization. The intrinsic activity of the brain reflects, in part, past activities, and these fluctuations impact future behavior (Sadaghiani and Kleinschmidt, 2013). Brain functionality and fluctuations are believed to determine and shape connectivity patterns. Here, we study the brain's intrinsic connectivity using resting-state functional connectivity MRI (rs-fcMRI) (Power et al., 2014b), which characterizes the functional relationship between brain regions while a participant is not performing a specific task by correlating slow spontaneous fluctuation of the blood oxygen level dependent (BOLD) signal. These intrinsic activity correlations can reveal the cohesive connections and interactions present in neuronal networks (Boly et al., 2008). Previous studies in adults have found that intrinsic brain connectivity within cortico-striatal networks were related to an individual's temporal discounting preference (Callusso et al., 2015; Li et al., 2013).

1.3. Development of brain networks underlying temporal discounting

It is hypothesized that differential rates of maturation across

cortico-striatal systems, and the protracted development of the interconnections between them, are related to changes in behavior across development (Casey, 2015; Costa Dias et al., 2012, 2015; van den Bos et al., 2015). In adults, it has been theorized that greater recruitment of control networks (and less recruitment of the valuation networks) are indicative of choosing the LLR, however, it is currently unclear if this brain-behavior relationship is present throughout development. One of the first task-based fMRI studies of temporal discounting examined the impact of age-related (ages 12–32 years; males) changes in brain activation when deciding between a SSR and a LLR (Christakou et al., 2011). This study demonstrated that when choosing an immediate reward, *increased* recruitment of the vmPFC and *decreased* recruitment of the ventral striatum, insula, anterior cingulate, occipital, and parietal cortices was related to increasing age and preference for LLR. Further, greater coupling between the ventral striatum and vmPFC was also related to increasing age and preference for LLR, suggesting that increased functional connectivity between the vmPFC and ventral striatum (regions of the valuation network) might be one neural mechanism underlying developmental changes in the preference for delayed rewards.

Another theory is that neural systems involved in three cognitive processes: valuation (i.e., the value placed on a certain stimuli or outcome), cognitive control (i.e., engaging in goal-directed cognitive processes), and prospection (i.e., thinking about the future), are involved in the process of temporal discounting (Peters and Büchel, 2011). Using this framework, Banich et al. (2013) compared the behavioral and neural correlates of temporal discounting in younger (14–15 years) and older (17–19 years) adolescents, and how these measures related to an individual's self-reported tendency to think beyond the present. Behaviorally, older adolescents were more likely to choose a delayed reward over an immediate reward, and were slower than younger adolescents to choose the immediate reward (Banich et al., 2013). The pattern of brain activity related to intertemporal decision making was more distinct when choosing between immediate versus delayed rewards in the older adolescents compared to the younger adolescents (Banich et al., 2013). Across groups, individuals who reported a greater tendency to think beyond the present showed decreased recruitment of cognitive control regions during the temporal discounting task. These results suggest that both age and individual differences are related to the neural processing of temporal discounting.

Another study found that greater white matter integrity in pathways connecting the frontal and temporal cortices with other areas of the brain were positively correlated with the preference for delayed rewards across ages 9–23 years (Olson et al., 2009). Some of these correlations were developmentally related, whereas some of the effects appeared to be age-independent. For example, the relationship between greater white matter integrity in right frontal and left temporal regions and increased preference for delayed reward was not attributable to age. However, the relationship between integrity of white matter in left frontal, right temporal, right parietal (as well as some subcortical-cortical circuits) and the preference for delayed reward was age-related, as these white matter tracts also increased in integrity across the age range studied. These results show that both age and individual differences in neural circuitry are related to an individual's preference for immediate versus delayed rewards. A recent longitudinal study examined the relationship between temporal discounting and fronto-striatal circuitry in individuals between the ages of 8–26 (Achterberg et al., 2016). This study found that preference for LLR increased non-linearly between childhood and early adulthood, and that greater fronto-striatal white matter integrity was related to the preference for LLR (Achterberg et al., 2016).

Taken together, these studies demonstrate that people, on average, show increasing preference to wait for larger rewards rather than take immediate (smaller) rewards as they get older, but the increase may be nonlinear. Individual differences across development in temporal discounting preference are related to differences in functional brain

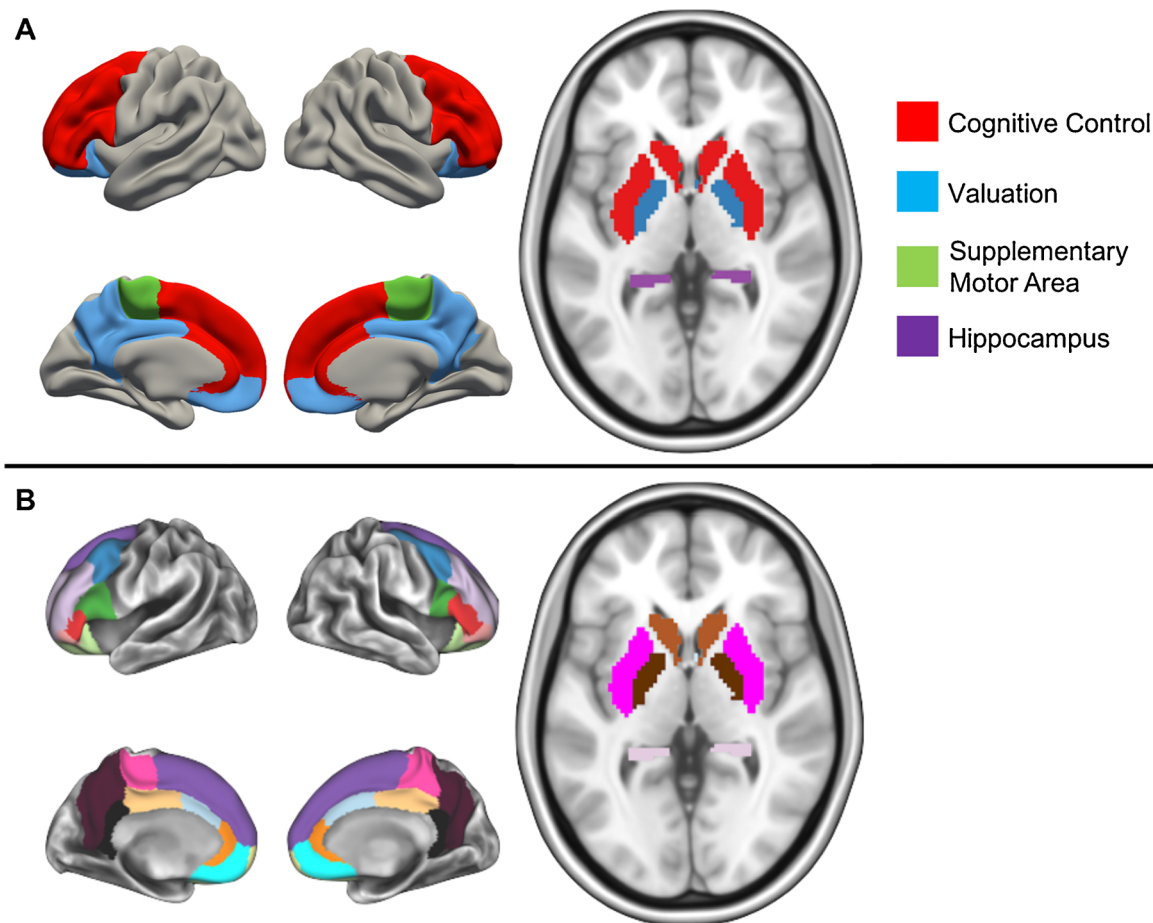


Fig. 1. Brain systems of interest and regions of interest. [A] Brain networks (including two other regions out of the networks) included in this study. The regions in red represent the cognitive control network. The regions in blue represent the valuation network. The regions in green and purple represent the supplementary motor area and the hippocampus, respectively. [B] Each brain region included in this study. (For interpretation of the references to color in this figure legend, the reader is referred to the web version of this article.)

organization. How one comes to choose a smaller immediate reward over a larger distant reward could be related to how that individual values the proposed reward, or it could be related to how well that individual can inhibit reflexive urges or the ability to think about the future. The development of brain systems involved in evaluating rewards, cognitive control, and thinking about the future all appear to contribute to the developmental changes in how we process situations that involve us making a choice between an immediate outcome and a distant outcome.

1.4. Current study

This current project examines how developmental changes in functional connectivity between and within the cognitive control network, valuation network, hippocampus and SMA relate to temporal discounting preferences during the transition into adolescence. Specifically, we examined if changes in functional connectivity strength could explain additional variance in temporal discounting preferences above chronological age. Previous studies have reported no significant difference in discounting behavior between boys and girls (Cross et al., 2011; Lee et al., 2013), suggesting that any sex effects are likely to be small. Therefore, to conserve statistical power, the relationship between sex and temporal discounting behavior was not examined.

2. Methods

2.1. Participants

Our two neurotypical samples were drawn from an ongoing longitudinal project examining brain development in children, recruited from the community, with and without attention-deficit/hyperactivity disorder (ADHD). Our first sample consisted of 64 individuals with 2 or 3 longitudinal scans each ($n = 137$ scans), and our second, cross-sectional, sample consisted of 84 individuals. Details for both samples are included in Table 1. All participants were typically-developing children without psychiatric diagnoses and exhibited typical neurological patterns of thoughts and behavior throughout the study. Psychiatric status was evaluated based on evaluations with the Kiddie Schedule for Affective Disorders and Schizophrenia (KSADS; Puig-Antich and Ryan, 1986) administered to a parent; parent and teacher Conners' Rating Scale-3rd Edition (Conners, 2003); and a chart review that required the agreement between a child psychiatrist and neuropsychologist. Any participant who was identified as having a current psychiatric, neurological, or neurodevelopmental disorder was excluded from the present study. IQ was estimated with a three-subtest short form (block design, vocabulary, and information) of the Wechsler Intelligence Scale for Children, 4th Edition (Wechsler, 2003).

Table 1
Participant demographic characteristics for each sample.

	Longitudinal Sample Characteristics			Cross-sectional Sample Characteristics		
	All	Female	Male	All	Female	Male
N	64	23	41	84	42	42
Age mean (SD)	10.8 (1.83)	10.6 (1.95)	10.9 (1.77)	10.3 (1.39)	10.3 (1.34)	10.3 (1.44)
Age range	7.3–15.7	7.3–15.7	7.5–14.5	7.3–13.3	8–13.3	7.2–13.2
AUC mean (SD)	0.51 (0.273)	0.51 (0.261)	0.51 (0.281)	0.45 (0.288)	0.44 (0.306)	0.47 (0.273)
AUC range	0.04–1	0.07–0.99	0.04–1	0.02–0.98	0.03–0.98	0.02–0.98
IQ mean (SD)	115.3 (13.95)	116.6 (9.58)	114.6 (15.88)	116.5 (13.82)	114.5 (14.86)	118.4 (12.59)
IQ range	72–144	98–132	72–144	78–148	78–144	96–148
N visits	137	49	88	84	42	42
2 visits	55	20	35	—	—	—
3 visits	9	3	6	—	—	—

2.2. Temporal discounting task

The temporal discounting task evaluates personal preference for a hypothetical delayed or immediate reward. Participants were presented a computerized task with a series of questions, and were read the following instruction before proceeding to the task:

For the next task, you can choose between two options by clicking on it using the computer mouse. You can change your selection as often as you would like. Once you have decided which option you prefer, you can go on to the next question by clicking on the ‘next question’ box. One option will always be some amount of money available now. The other option will always be some amount of money later. The waiting period will vary between now and 180 days. Imagine that the choices you make are real— that if you choose ‘money now’ you would receive that amount of money at the end of the task and that if you choose ‘money later’ that you would actually have to wait before receiving the money. So, what are you going to do?

The computer-based task consisted of 92 questions with an option to get a smaller reward immediately or get a larger amount of money (\$10.00) at a later time period. Most of the participants were presented delays in intervals of 7, 30, 90, 180 days; a small percent of the participant were presented with different delay intervals of 1, 7, 30, 90 days.

Our temporal discounting task was analyzed by multivariate mathematical equations to measure an individual’s decision-making preference. Reward in relation to the time span is usually used to measure the preference of an individual or a collective population generalized by age.

There are many mathematical ways to analyze temporal discounting task, however, for this experiment we choose Area Under Curve (AUC). AUC (see Box 1) best represents the preference of the participants as it takes into consideration the indifference point and the corresponding delay time (Myerson et al., 2001). AUC is equated to best represent the variables present in this experiment; it takes into account the sum of indifference and delay points acquired through temporal discounting, and outputs one value making it easier for analysis (Myerson et al., 2001).

The x_2 and x_1 are the delayed points, and y_2 and y_1 represent the indifference points that correspond to the delays (Hamilton et al., 2015; Odum, 2011). The AUC outputs a signal value between 0 and 1; a lower number represents less tolerance for the delay time and greater

possibility to disregard the value of the reward (Myerson et al., 2001; Odum, 2011). The closer the AUC value is to zero, the more temporal discounting is present, and therefore the participant is less likely to wait for a larger reward. Likewise, the farther away the AUC value is to zero, the more likely the participant is going to wait for the larger reward to be received at a later time.

Three validity criteria were applied to the quantification of AUC. The first criterion was to make sure that an indifference point for a specific delay was not greater than the preceding delay indifference point by more than 20% or \$2 (Johnson and Bickel, 2008). The next criterion was the requirement for the final indifference point, at 180 days, to be less than the first indifference point, at 0 days, to indicate variation in subjective value of rewards across (Johnson and Bickel, 2008). The final criterion was to require the first indifference point, at 0 day, to be at least 9.25. This last criterion was enforced because a lower value indicates that the participant chose multiple time to receive the smaller “now” over the larger “now”, suggesting poor task engagement or misunderstanding of the task (Mitchell et al., 2015).

2.3. MRI acquisition

MRI was acquired using a 3.0 T Siemens Magnetom Tim Trio scanner with a twelve-channel head-coil at the Oregon Health & Science University Advanced Imaging Research Center. One high-resolution T1-weighted MPRAGE (TR = 2300 ms, TE = 4 ms, FOV = 240 × 256 mm, 1 mm isotropic, sagittal acquisition) and multiple T2-weighted echo planar imaging (TR = 2500 ms, TE = 30 ms, FOV = 240 × 240 mm, 3.8 mm isotropic, either 82 or 120 volumes, axial acquisition, 90° flip angle) series were acquired during each scan visit. Functional data were collected at rest, in an oblique plane (parallel to anterior commissure-posterior commissure plane), and steady state magnetization was assumed after five frames (~10 s). Participants were instructed to stay still and fixate their gaze on a standard fixation-cross in the center of the display during the acquisition of resting state scans.

2.4. Image processing

The data were processed following the minimum processing steps outlined by the Human Connectome Project (Glasser et al., 2013), which included the use of FSL (Jenkinson et al., 2012; Smith et al., 2004; Woolrich et al., 2009) and FreeSurfer image analysis suite (<http://surfer.nmr.mgh.harvard.edu/>) (Dale et al., 1999; Fischl et al., 1999). With this method, gradient distortion corrected T1w and T2w

Box 1
AUC Equation.

$$AUC = \sum (x_2 - x_1) \left| \frac{y_1 - y_2}{2} \right|$$

volumes are first aligned to MNI's AC-PC axis and then nonlinearly normalized to the MNI atlas. Next, the T1w and T2w volumes are re-registered using boundary based registration (Greve and Fischl, 2009) to improve alignment. The brain of each individual is then segmented using the 'recon-all' FreeSurfer functions, which are further improved by utilizing the enhanced white matter-pial surface contrast of the T2w sequence. The initial pial surface is calculated by finding voxels that are beyond ± 4 standard deviations from the grey matter mean. The resulting parameter is then used to make sure no lightly myelinated grey matter is excluded. The estimated segmentation is refined further by eroding it with the T2w volume. Of the 221 total scan visits included in this study, 51 (23%) were processed without a T2w volume, either because this sequence was not acquired or was judged as being of low quality. These 51 were processed using FreeSurfer's regular T1 segmentation algorithm (Fischl et al., 2002). Next, the preliminary pial surface and white matter surface are used to define an initial cortical ribbon. The original T1w volume is smoothed with the ribbon using a Gaussian filter with a sigma of 5 mm. Then, the original T1w image is divided by the smoothed volume to account for low frequency spatial noise. This filtered volume is used to recalculate the pial surface, but now using 2 (instead of 4) standard deviations as threshold to define the pial surface. These segmentations are then used to generate an individualized 3D surface rendering of each individual, which is finally registered to the Conte 69 surface atlas as defined by the Human Connectome Project. This registration process allows all data types (cortical thickness, grey matter myelin content, sulcal depth, function activity, functional and structural, connectivity, etc.) to be aligned directly within and between individuals. All T1w and T2w MRI scans were quality controlled for any noticeable movement through visual inspection of raw and reconstructed images. The images were assessed in a pass or fail manner; scans that failed were excluded from the samples included in the present study.

Functional EPI data are registered to the first volume using a 6-degrees of freedom linear registration and corrected for field distortions (using FSL's TOPUP), except for two scans (of 221) where no field map had been acquired. Next the EPI volumes are averaged, with each volume of the original time series re-registered to the average EPI volume using a 6-degrees of freedom linear registration. This last step avoids biases due to a single frame being used, which may be confounded by variability of movement across a given run. The average EPI volume is then registered to the T1w volume. The matrices from each registration step are then combined, such that each frame can be registered to the atlas all in a single transform (i.e. only one interpolation).

The resulting time-courses are then constrained by the grey matter segmentations and mapped into a standard space of 91,282 surface anchor points (greyordinates). This process accounts for potential partial voluming by limiting the influence of voxels that "straddle" grey and non-grey matter voxels (pial surface, white matter, ventricles, vessels, etc). Two thirds of the greyordinates are vertices (located in the cortical ribbon) while the remaining greyordinates are voxels within subcortical structures. Thus, the BOLD time courses in greyordinate space are the weighted average of the volume's time courses in grey matter, where the weights are determined by the average number of voxels wholly or partially within the grey matter ribbon. Voxels with a high coefficient of variation are excluded. Next, the surface time courses are downsampled to the greyordinate space after smoothing them with a 2 mm full-width-half-max Gaussian filter.

The additional preprocessing steps necessary for resting-state functional connectivity analyses consist of regressing out the whole brain (in this case the average signal across all greyordinates (e.g., see Burgess et al., 2016), ventricle and white matter average signal, and displacement on the 6 motion parameters, their derivatives and their squares (Power et al., 2014a). All regressors are individualized and specific to the participant, based on their own segmentations. The regression's coefficients (beta weights) are calculated solely on the frames where the frame displacement is below 0.3 mm to reduce the influence

of movement "outliers" on the output data, but all the time courses are regressed to preserve temporal order for temporal filtering. Finally, time courses are filtered using a first order Butterworth band pass filter with cutting frequencies of 9 mHz and 80 mHz.

We applied a strict motion censoring procedure to the resting-state images (Fair et al., 2012b; Power et al., 2012) which takes the absolute value of the backward-difference for all rotation and translation measures in millimeters, assuming a brain radius of 50 mm, and summates those absolute backward-differences for a measure of overall framewise displacement (FD). Volumes with a displacement exceeding 0.2 mm were excluded, and we also removed frames with less than five contiguous frames of low motion data between instances of high motion ($FD > 0.2$ mm) data to confidently account for motion effects on adjacent volumes (Power et al., 2014a). Only participants with greater than 5 min of high quality data were included in the present analysis. The mean framewise displacement of participants in the first sample was 0.08 ± 0.02 mm; range 0.05–0.13 mm. The mean framewise displacement of participants in the second sample was 0.09 ± 0.02 mm; range 0.04–0.13 mm. More information on the motion characteristics on the full sample (i.e. including those excluded) can be viewed in Dosenbach et al., (2017).

2.5. Regions of interest

Our regions of interest (ROIs) included regions within valuation and cognitive control systems, as well as hippocampus and supplementary motor area (SMA). For our cortical ROIs, we selected regions within each of these networks from the Desikan-Killiany atlas provided by FreeSurfer (Desikan et al., 2006). While other parcellations can be considered, we chose this parcellation in order to examine anatomically-defined cortical regions that have been identified in previous work. Cortical reconstruction and volumetric segmentation was performed with the FreeSurfer image analysis suite, which is documented and freely available for download online (<http://surfer.nmr.mgh.harvard.edu/>). The technical details of these procedures are described in prior publications (Dale et al., 1999; Fischl et al., 2002; Fischl and Dale, 2000). FreeSurfer uses individual cortical folding patterns to match cortical geometry across subjects (Fischl et al., 1999), and maps this parcellation of the cerebral cortex into units with respect to gyral and sulcal structure (Desikan et al., 2006; Fischl et al., 2004). Our striatal and subcortical ROIs were defined based on FreeSurfer's anatomical segmentation procedure. For the purposes of this study, we examined the nucleus accumbens (NAcc), pallidum, amygdala, medial orbitofrontal cortex (mOFC), and posterior cingulate cortex (PCC) as part of the valuation network, and the caudate, putamen, anterior cingulate cortex (ACC), dorsal anterior cingulate cortex (dACC), dorsolateral prefrontal cortex (dlPFC), inferior frontal gyrus (IFG), and ventrolateral prefrontal cortex (vlPFC) of the cognitive control network (Fig. 1; SI Table 1).

2.6. Statistical analysis

In this study, we first tested to see whether chronological age could be used to predict temporal discounting preference as measured by AUC. We then tested to see if the strength of connectivity between each of our ROIs was able to explain variance in temporal discounting AUC values above chronological age. All analyses were conducted in R version > 3.3.3 (<https://www.r-project.org/>). The script we used to conduct these analyses is freely available online to facilitate reproducibility and replication efforts (https://github.com/katemills/temporal_discounting).

2.7. Sample 1

For our first, longitudinal, sample we tested each of these questions using mixed-effects models with the *nlme* package implemented

Table 2
Comparison of polynomial age models for the longitudinal sample.

Longitudinal sample								
	Model	df	AIC	BIC	logLik	Test	L.Ratio	p-value
Null Model	1	3	25.0	33.7	-9.5			
Linear age	2	4	18.8	30.4	-5.4	1 vs 2	8.2	0.0042
Quadratic age	3	5	15.8	30.4	-2.9	2 vs 3	5.0	0.0257
Cubic age	4	6	15.4	32.9	-1.7	3 vs 4	2.4	0.1226

through R. Mixed effects modeling accounts for the non-independence of the data collected from the same individual over time and allows for unequal spacing between data collection points. This statistical analysis contains both the average slope and intercepts of the parameter (fixed effects), and varying intercept for each individual that is a random deviation of the fixed effect (random effect). We tested the following three polynomial models to predict AUC from chronological age:

$$\text{Linear age model: } y = \beta_0 + \beta_1(x)$$

$$\text{Quadratic age model: } y = \beta_0 + \beta_1(x) + \beta_2(x^2)$$

$$\text{Cubic age model: } y = \beta_0 + \beta_1(x) + \beta_2(x^2) + \beta_3(x^3)$$

Where y is the AUC value, and β_0 represents the intercept; x represents the participant's age; and β_1 , β_2 and β_3 represent regression coefficients. We centered age for all analyses (10.70 years). The three age models were compared and tested against a null model that only included the random intercept for each individual. The best fitting model was determined by Akaike Information Criterion (AIC) and likelihood ratio (LR) statistics using the heuristic of parsimony. The model with the lowest AIC value that was significantly different ($p < .05$), as determined from LR tests, from less complex models was chosen.

To identify the connections that could predict an individual's AUC score above chronological age, we used LR statistics to compare models including a connection of interest (COI) correlation coefficient as an interaction and/or main effect added to the age only model. These brain connectivity models were then compared against each other as well as the best fitting age model. The model with the lowest AIC value that was significantly different ($p < .01$) from less complex models was selected as the best fitting model. To account for the possibility that brain connectivity alone could account for more variance in AUC values than the age-only model or the multivariate models, we also tested to see if a model including the COI correlation coefficient, but not age, was the best fitting model. We identified connectivity-only models if they had lower AIC than the age only models, and were also both significantly different and had lower AIC than the other more complex models. Finally, we examined if including key covariates measures such as IQ, puberty, or race impacted these models (see Supplementary methods).

2.8. Sample 2

We examined the same questions in the second sample to test the replicability of the results obtained from the first sample. As we wanted to examine the generalizability of the effects and developmental trends observed in our first sample, we set out to test the relevant connections observed from the analysis of the first sample in a cross-sectional sample with a similar, but not identical, age range. Further, by testing the relevant connections observed from the analysis of the first sample in this second, independent, sample reduces the likelihood of reporting false positives.

Similar to our first sample, we first examined the relationship between AUC and chronological age, specifically by comparing linear to nonlinear models (quadratic & cubic). Since these data were cross-sectional, we used regular linear regression to fit these models and

compared models through F tests ($p < .05$). Age was centered for all analyses (10.23 years). Once the best age model was determined, we tested if adding COI correlation coefficients to the model would improve the model fit through F tests ($p < .05$). We only examined the COIs that were determined to explain additional variance in AUC above age in the first sample. As with the longitudinal sample, we examined if including key covariates measures such as IQ, puberty, or race impacted these models (Supplementary methods).

2.9. Developmental analysis

To test whether developmental changes in functional connectivity within relevant COIs could predict future temporal discounting preference, we performed a *post-hoc* linear regression analysis with baseline AUC, change in functional connectivity, and age at the second time point as predictors for AUC at the second timepoint (see Supplementary methods). To assess if developmental changes in connectivity were more informative for predicting future temporal discounting preference at certain ages, we also examined the interaction between change in functional connectivity and age at the second time point. The models were only conducted for the relevant COIs identified in the previous analyses, and only for the participants in the longitudinal sample. Models were compared with F tests ($p < .05$).

3. Results

3.1. AUC increases from late childhood into early adolescence

Model comparisons between the null, linear age, quadratic age, and cubic age models are presented in Table 2. Of the three age models tested, the quadratic model best represented the relationship between age and AUC in this longitudinal sample (LR quadratic model vs. null: 13.2, $p < .002$). The results of this model suggest that, on average, each yearly increase in age across this sample was associated with an increase of 0.04 AUC, with a negative rate of change (-0.01) (Table 3; Fig. 2). These results should be interpreted from the predicted intercept at age 10.70 years (0.55). The graph illustrates a group-level increase in AUC until age ~11 years, but relative stability in AUC between ages 11–14 years.

In our second, cross-sectional, sample, we found evidence for a linear relationship between age and AUC (Fig. 2; blue). The linear model for this sample suggests that, on average, each yearly increase in age across this sample was associated with an increase of 0.05 AUC (Table 3; Fig. 2). These results should be interpreted from the predicted intercept at age 10.23 years (0.45). Overall, the graph shows a similar increase in AUC across the age period studied as is visible in the longitudinal sample.

3.2. Brain connectivity explains variance in AUC not accounted for by age

In the first sample, we found that AUC was best predicted by models including both age and connectivity for fifty-eight COIs (SI Table 2). Many of the connections (40%) were between regions within the cognitive control network, whereas 10% of connections were between regions within the valuation network. 36% of the connections were

Table 3

Fixed effects for best fitting (quadratic) age model predicting AUC for the longitudinal sample.

Longitudinal Sample					
	Value	Std. Error	DF	t-value	p-value
Intercept	0.55	0.03	71	17.0	< 0.0001
Linear age	0.04	0.01	71	3.2	0.0021
Quadratic age	-0.01	0.01	71	-2.2	0.0291

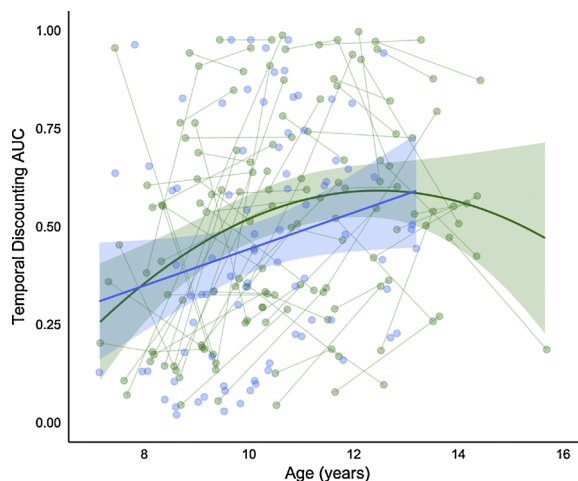


Fig. 2. Best fitting age models for AUC. The green line represents the predicted model fit for AUC for sample 1 (longitudinal sample) and the blue line represents the predicted model fit for AUC for sample 2 (cross-sectional sample). Shading represents the 95% confidence intervals. Raw data are plotted in the background, with each individual measurement represented by a circle, and lines connecting data collected from the same individual across time. (For interpretation of the references to color in this figure legend, the reader is referred to the web version of this article.)

between the cognitive control network regions and the valuation network regions. None of the identified connections included connections between the control network and the SMA or the hippocampus, however, one connection between the valuation network and hippocampus and three connections between the valuation and the SMA were identified as relevant to predicting AUC. All four possible connections between the SMA and hippocampus were identified as relevant to predicting AUC.

Of the fifty-eight connections identified in the first sample, only nine were replicated in the cross-sectional sample (Table 4; Fig. 3). Three of the nine connections represented connections within regions of the cognitive control system (left dlPFC – right dACC; bilateral dlPFC; bilateral superior frontal cortex); three represented connections within regions of the valuation system (right pallidum – left PCC; right pallidum – right PCC; right mOFC – left amygdala); and three represented connections between these two systems (left dlPFC – right PCC; left superior frontal cortex – right PCC; left mOFC – right vLPFC). Model statistics for these nine models are detailed for both the longitudinal sample and cross-sectional sample in Table 4. Neither the best fitting models, nor the effects of interest, were impacted by the inclusion of IQ as a covariate, and the inclusion of puberty or race as a covariate had a minimal impact, if any, on the models and effects of interest (Supplementary Table 3).

The majority of the identified connections showed similar effects across samples. The three connections within the cognitive control system impacted the prediction of AUC similarly in both samples: individuals with greater connectivity strength between these cognitive control regions were predicted to have a preference for LLR (higher AUC) across the age ranges studied. The beta values for the main effect of connectivity were similar across the samples as well, with connectivity beta estimates ranging from 0.26–0.37 for the longitudinal sample, and 0.30–0.42 for the cross-sectional sample.

The three connections within the valuation system also impacted the prediction of AUC similarly in both samples: individuals with greater connectivity strength between these valuation regions were predicted to have a preference for the SSR (lower AUC) across the age ranges studied. The beta values for the main effect of connectivity were similar across the samples as well, with connectivity beta estimates ranging from −0.38 to −0.23 for the longitudinal sample, and −0.58

to −0.27 for the cross-sectional sample. The impact of connectivity between the right pallidum and PCC on predicting AUC with age was virtually identical for both cortical hemispheres.

Individuals with greater connectivity strength between the left mOFC and right vLPFC were predicted to have a preference for LLR (higher AUC) across the age ranges studied, similar to patterns found for connections between the cognitive control regions. Connectivity between these two regions was a better predictor of AUC than age alone in the cross-sectional sample. Within the longitudinal sample, connectivity strength between the right PCC and the left dlPFC or left superior frontal cortex interacted with the quadratic age term to predict AUC, with stronger connectivity strength predicting a preference for LLR (higher AUC) only at the tail ends of the age range. Within the cross-sectional sample, participants with greater connectivity strength between the right PCC and left dlPFC were predicted to have a preference for LLR (higher AUC). Connectivity between the right PCC and left superior frontal cortex was a better predictor of AUC than age alone in the cross-sectional sample, with individuals with greater connectivity strength between these regions showing a preference for LLR (higher AUC).

3.3. Developmental analysis

We found that, in addition to baseline AUC, developmental changes in functional connectivity between three of the nine identified connections were able to predict subsequent AUC (Supplementary Table 4). Increased strength between the left dlPFC and right dACC across time was associated with increased preference for waiting for LLR, whereas the opposite developmental finding was observed for connectivity between the right PCC and right pallidum. This is in line with our finding that increased strength between cognitive control regions, and decreased strength between valuation system regions, is related to increased preference for LLR in the transition into adolescence. Further, developmental changes in connectivity strength between the left amygdala and right mOFC interacted with the age of the participant at the second timepoint to explain variance in future temporal discounting after controlling for baseline temporal discounting preference.

4. Discussion

In this study, we investigated whether individual differences in functional brain organization are associated with temporal discounting preferences in the transition into adolescence. Specifically, we tested if functional connectivity between regions involved in valuation and cognitive control, as well as the hippocampus and SMA, could explain variance in temporal discounting preference (AUC) above chronological age. To ensure validity of our reported results, we tested these models in two independent datasets: a longitudinal dataset of children aged 7–15 years and a cross-sectional dataset of 7–13 year olds.

In both samples, longitudinal and cross-sectional, we observed a group-average increase in AUC between late childhood and early adolescence. We found evidence that the relationship between age and AUC was best represented by a quadratic trajectory in our longitudinal sample, with AUC increasing between ages 7–11 years before stabilizing. For the cross-sectional sample, we identified a linear increase in AUC between ages 7–13 years. While the best fitting model differed between these samples, the overall pattern observed in both samples reflected a general trend for our participants to prefer waiting for a later, larger reward (LLR) as they got older.

This result supports the theory that temporal discounting preferences shift in the transition into adolescence (Achterberg et al., 2016; Scheres et al., 2014). Scheres et al., (2014) demonstrated in a cross-sectional sample encompassing ages 6–19 years that adolescents were more likely to wait for the LLR in comparison to children and young adults. Achterberg et al., (2016) similarly found that the ability to delay gratification increased from childhood into adolescence. It is important

Table 4
Best fitting model characteristics for the nine connections of interest that replicated across the both samples.

Connection	Networks	Longitudinal sample						Cross-sectional sample		
		Best Fit Model	LR test	AIC diff.	Intercept (SE)	Linear age Estimate (SE)	Quadratic age Estimate (SE)	Connectivity Estimate (SE)	Quadratic age x Connectivity (SE)	
Left dlPFC – Right dACC	Control – Control	main effect	$\chi^2(1) = 7.13, p = 0.0076$	5.13	0.59 (0.03)	0.05 (0.01)	-0.01 (0.01)	0.26 (0.1)	—	
Left dlPFC – Right dlPFC	Control – Control	main effect	$\chi^2(1) = 8.68, p = 0.0032$	6.68	0.4 (0.06)	0.05 (0.01)	-0.01 (0.01)	0.36 (0.12)	—	
Left Superior Frontal Cortex – Right Superior Frontal Cortex	Control – Control	main effect	$\chi^2(1) = 8.95, p = 0.0028$	6.95	0.36 (0.07)	0.05 (0.01)	-0.01 (0.01)	0.37 (0.12)	—	
Right Pallidum – Right PCC	Valuation – Valuation	main effect	$\chi^2(1) = 8.27, p = 0.004$	6.27	0.56 (0.03)	0.05 (0.01)	-0.01 (0.01)	-0.34 (0.11)	—	
Right Pallidum – Left PCC	Valuation – Valuation	main effect	$\chi^2(1) = 8.74, p = 0.0031$	6.74	0.54 (0.03)	0.05 (0.01)	-0.01 (0.01)	-0.38 (0.12)	—	
Right mOFC – Left Amygdala	Valuation – Valuation	quadratic interaction	$\chi^2(2) = 9.97, p = 0.0069$	5.97	0.59 (0.04)	0.04 (0.01)	-0.02 (0.01)	-0.23 (0.15)	0.09 (0.03)	
Left dlPFC – Right PCC	Control – Valuation	quadratic interaction	$\chi^2(2) = 11.44, p = 0.0033$	7.44	0.54 (0.03)	0.06 (0.01)	-0.01 (0.01)	-0.08 (0.11)	0.1 (0.03)	
Left Superior Frontal Cortex – Right PCC	Control – Valuation	quadratic interaction	$\chi^2(2) = 9.9, p = 0.0071$	5.9	0.55 (0.03)	0.06 (0.01)	-0.01 (0.01)	-0.2 (0.12)	0.1 (0.03)	
Left mOFC – Right vIPFC	Valuation – Control	main effect	$\chi^2(1) = 7.13, p = 0.0076$	5.13	0.51 (0.04)	0.04 (0.01)	-0.01 (0.01)	0.27 (0.1)	—	
Cross-sectional sample										
Connection	Networks	Best Fit Model	F test	adj R Sq	Intercept (SE)	Linear age (SE)	Connectivity (SE)	Connectivity (SE)	Connectivity (SE)	Connectivity (SE)
Left dlPFC – Right dACC	Control – Control	main effect	$F(2,81) = 5.13, p = 0.0203$	0.09	0.51 (0.04)	0.05 (0.02)	0.3 (0.13)	0.42 (0.18)	0.4 (0.18)	
Left dlPFC – Right dlPFC	Control – Control	main effect	$F(2,81) = 4.99, p = 0.0233$	0.09	0.28 (0.08)	0.05 (0.02)	0.25 (0.1)	0.4 (0.18)	0.4 (0.18)	
Left Superior Frontal Cortex – Right Superior Frontal Cortex	Control – Control	main effect	$F(2,81) = 4.92, p = 0.025$	0.09	0.46 (0.03)	0.04 (0.02)	-0.53 (0.19)	-0.58 (0.2)	-0.58 (0.2)	
Right Pallidum – Right PCC	Valuation – Valuation	main effect	$F(2,81) = 6.21, p = 0.007$	0.11	0.45 (0.03)	0.05 (0.02)	0.47 (0.03)	0.05 (0.02)	-0.27 (0.12)	
Right Pallidum – Left PCC	Valuation – Valuation	main effect	$F(2,81) = 6.72, p = 0.0043$	0.12	0.48 (0.03)	0.05 (0.02)	0.48 (0.03)	0.05 (0.02)	0.28 (0.14)	
Right mOFC – Left Amygdala	Control – Valuation	main effect	$F(2,81) = 4.62, p = 0.0342$	0.08	0.44 (0.03)	0.05 (0.02)	-0.37 (0.15)	-0.35 (0.14)	—	
Left dlPFC – Right PCC	Control – Valuation	coi only	$F(1,82) = 6.18, p = 0.015$	0.06	—	—	—	—	—	
Left Superior Frontal Cortex – Right PCC	Control – Valuation	coi only	$F(1,82) = 6.27, p = 0.0142$	0.06	0.41 (0.03)	—	—	—	—	

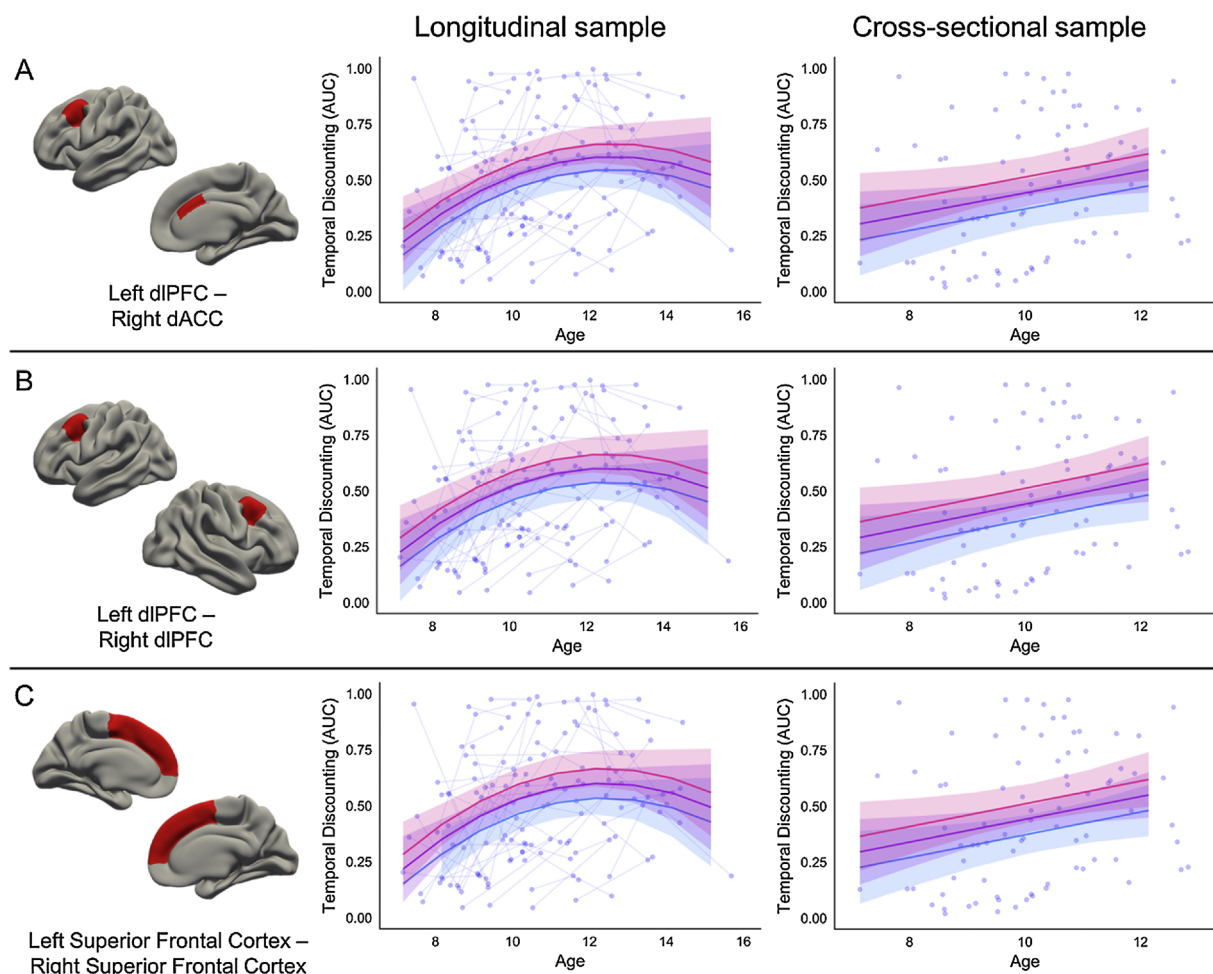


Fig. 3 a–c. Relationship between cognitive control regions and AUC. The cortical regions involved in the connectivity between two cognitive control systems are represented by red on the brain. Pink trajectory represents AUC for an individual with 1 standard deviation higher connectivity than the mean between the two regions. Purple trajectory represents predicted AUC for participants with the mean connectivity strength between the two regions. Blue trajectory represents AUC for an individual with 1 standard deviation lower connectivity than the mean between the two regions. Raw data are plotted in the background, with each individual measurement representing a circle, and lines connecting data collected from the same individual across time. (For interpretation of the references to color in this figure legend, the reader is referred to the web version of this article.)

to note that, although we found a group-average increase in AUC across the transition into adolescence, there was substantial individual variability (see Fig. 2). Further, because our sample age range ends at 15 years we cannot be sure if the preference for LLR declines between mid-to-late adolescence.

4.1. Individual differences in functional connectivity are related to temporal discounting preference

The current study proposed that individual variability in temporal discounting preference could be explained by differences in functional brain organization. To test this hypothesis, we examined if intrinsic functional connectivity between a set of *a priori* regions of interest and networks could improve the “age only” models in predicting an individual’s temporal discounting preference. To mitigate false positives and overfitting, we implemented both a stringent model selection procedure utilizing AIC as well as Likelihood Ratio tests paired with replication in an independent sample. We found nine distinct brain connections were able to explain variance in temporal discounting preference above age alone in both our longitudinal and cross-sectional samples. These findings suggest that individual differences in functional brain connectivity can explain individual variability in temporal discounting preferences during the transition to adolescence.

Our results demonstrate that individuals with greater connectivity

between cortical regions within cognitive control systems are more inclined to choose LLR. Specifically, we found that greater connectivity between the left dIPFC and the right dACC, bilateral dlPFC, and bilateral superior frontal cortex, relate to a preference for LLR for individuals across the transition into adolescence (Fig. 3a–c). Our post-hoc analysis revealed that developmental increases in connectivity strength between the left dIPFC and right dACC across the transition into adolescence was associated with increased preference for waiting for LLR.

Across samples, we found evidence that greater connectivity between right pallidum and the bilateral PCC was associated with a preference for SSR across the transition into adolescence. Specifically, greater connectivity between these valuation regions predicted lower AUC for individuals across the age ranges studied (Fig. 3d and e). These results align with previous findings showing individual differences in cortico-striatal circuitry are related to temporal discounting preferences (van den Bos et al., 2014, 2015). Our post-hoc analysis revealed that developmental decreases in connectivity strength between the right pallidum and right PCC across the transition into adolescence was associated with increased preference for waiting for LLR.

Our results also demonstrate that greater connectivity between the left amygdala and right mOFC was related to increased preference for the SSR in the transition to adolescence (Fig. 3f). While a main effect was found for the cross-sectional sample, there was an interaction

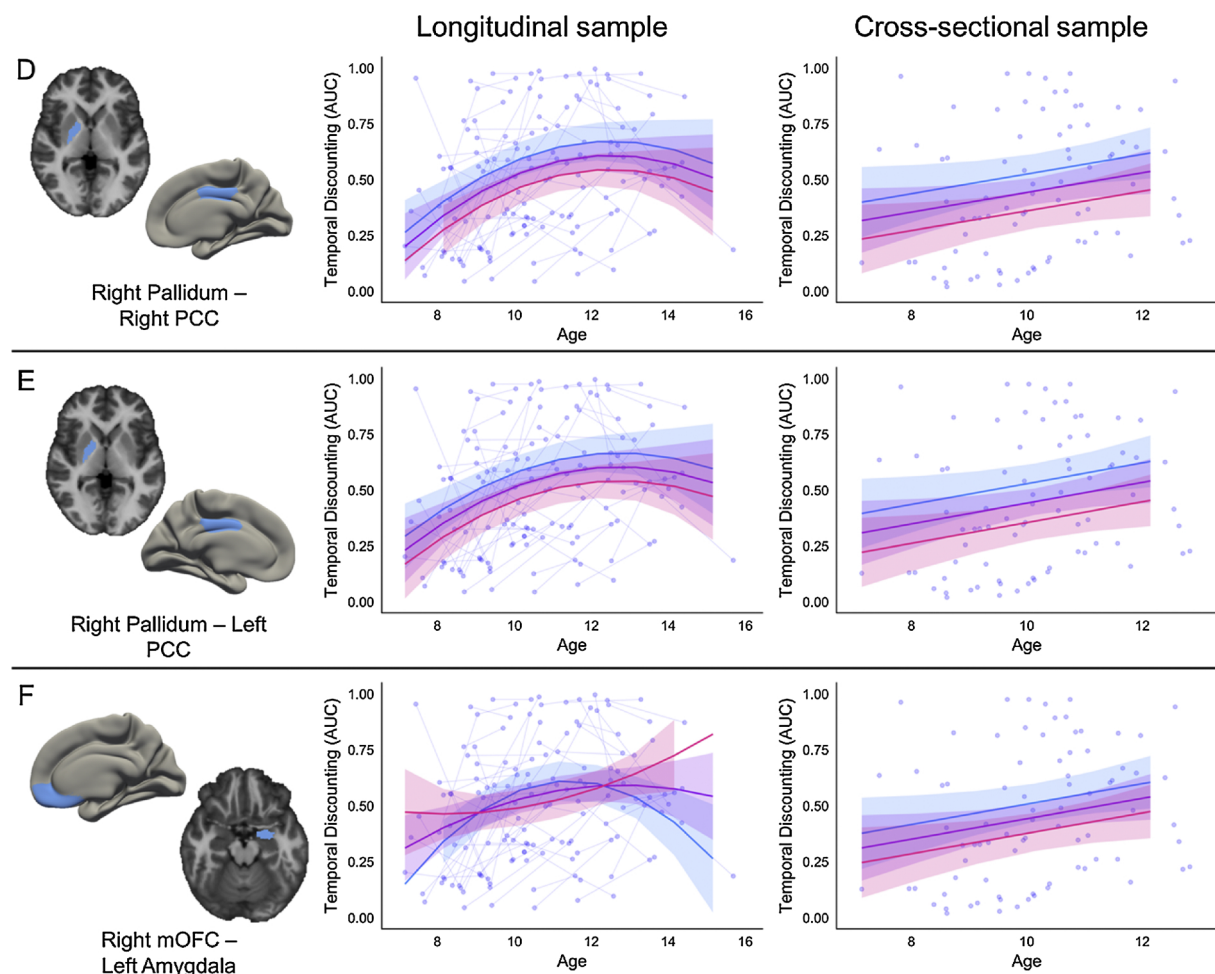


Fig. 3 d-f. Relationship between valuation regions and AUC. The cortical and subcortical regions involved in the connectivity between two valuation systems are represented by blue on the brain. Pink trajectory represents AUC for an individual with 1 standard deviation higher connectivity than the mean between the two regions. Purple trajectory represents predicted AUC for participants with the mean connectivity strength between the two regions. Blue trajectory represents AUC for an individual with 1 standard deviation lower connectivity than the mean between the two regions. Raw data are plotted in the background, with each individual measurement representing a circle, and lines connecting data collected from the same individual across time. (For interpretation of the references to color in this figure legend, the reader is referred to the web version of this article.)

between connectivity and the quadratic age term for the longitudinal sample. This presents the possibility that the relationship between greater connectivity between the left amygdala and right mOFC and temporal discounting preference is not static across ages 7–15 years. Indeed, our post-hoc analysis demonstrated that developmental changes in connectivity strength between the left amygdala and right mOFC interacted with the age of the participant at the second timepoint to explain variance in future temporal discounting after controlling for baseline temporal discounting preference. While increased strength between the left amygdala and right mOFC across time was generally related to increased preference for later larger rewards, this negatively interacted with age at the second time point. This suggests that the strengthening of these two valuation regions is related to increased preference for later larger rewards for younger participants.

Previous cross-sectional work has found evidence suggesting that age-related increases in connectivity between the ventral striatum and vmPFC is related to increasing preference for LLR (Christakou et al., 2011). While the results from the present analysis did not demonstrate this same developmental effect between these two specific regions, the results from our post-hoc analysis suggest that increased connectivity between subcortical-cortical regions of the valuation network might be a mechanism underlying developmental changes in the preference for delayed rewards. We found that developmental increases in connectivity between the pallidum and PCC, as well as between the

amygdala and mOFC, predicted a maturational shift to prefer LLR. In addition, the effect of increased connectivity between the amygdala and mOFC interacted with age in predicting developmental changes in temporal discounting preference, which suggests that older participants with increased connectivity prefer the SSR. This finding suggests that developmental increases in connectivity strength between those regions are predictive of increased preference for the LLR in late childhood, however, as participants get older, the pattern is reversed. This could be due to the differences in the regions that are age driven (van den Bos et al., 2015). Increased white matter integrity in fronto-striatal tracts between late childhood and early adulthood is related to increased preference for LLR (Achterberg et al., 2016). This is in keeping with our post-hoc interaction found between the amygdala and mOFC. However, in our study, rather than finding fronto-striatal tracts to be predictive of temporal discounting, we found the fronto-limbic tracts were of greater relevance in predicting later temporal discounting behavior.

While we found evidence that greater connectivity between the right PCC and the left dlPFC or left superior frontal cortex was related to greater preference for LLR for individuals across ages in the cross-sectional sample, the best fitting models in the longitudinal sample suggested a nonlinear relationship between this strength of these connections and AUC preference across age (Fig. 3g and h). We found that greater connectivity between the left mOFC to right vIPFC (the pars orbitalis region of the inferior frontal gyrus) was related to increased

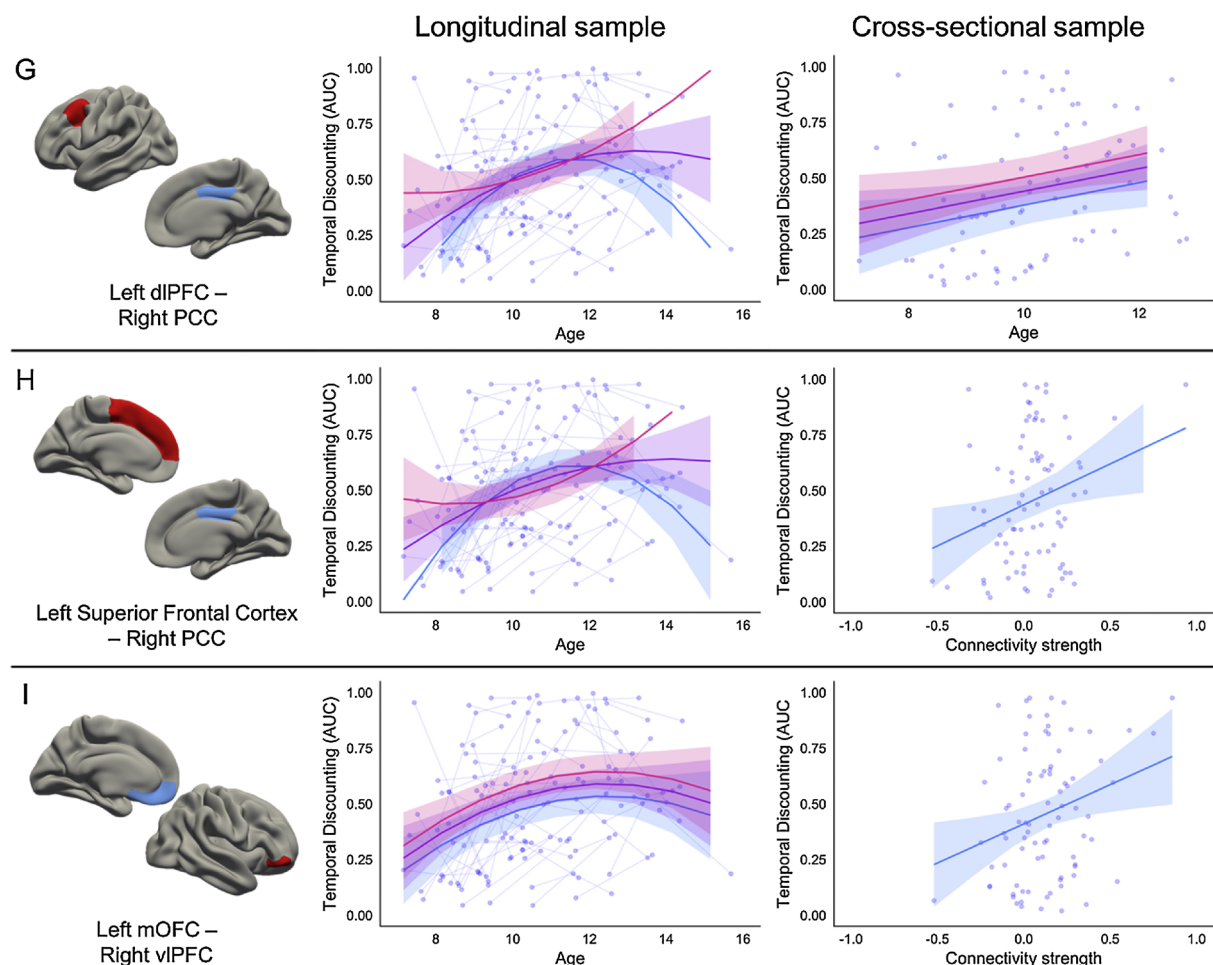


Fig. 3 g-i. Relationship between valuation network and cognitive control network and AUC. The cortical regions involved in the connectivity between valuation system and cognitive control system are represented by blue and red, respectively, on the brain. Pink trajectory represents AUC for an individual with 1 standard deviation higher connectivity than the mean between the two regions. Purple trajectory represents predicted AUC for participants with the mean connectivity strength between the two regions. Blue trajectory represents AUC for an individual with 1 standard deviation lower connectivity than the mean between the two regions. Raw data are plotted in the background, with each individual measurement representing a circle, and lines connecting data collected from the same individual across time. (For interpretation of the references to color in this figure legend, the reader is referred to the web version of this article.)

preference for LLR across the transition into adolescence. This possibly reflects that stronger functional connectivity at rest between these regions reflects the ability for the vIPFC/IFG to regulate mOFC signaling (Hare et al., 2009). In both samples, a main effect of greater connectivity between the dIPFC and several regions predicted higher AUC (increased preference for LLR or less discounting) for individuals across the transition into adolescence. This result held for connections between the dIPFC and dACC, bilateral dIPFC, as well as dIPFC and PCC, further underscoring the role of dIPFC in the development of temporal discounting behavior (Wang et al., 2017).

4.2. Role of dopaminergic signaling in temporal discounting behavior

All of the identified relevant connections between regions of the valuation network (amygdala, mOFC, PCC, and pallidum) showed a negative relationship with AUC, with stronger connectivity predicting a greater preference for SSR across participants. This could be related to the abundance of dopaminergic signaling in the valuation network. Multiple studies have shown that areas of the brain with dopaminergic innervation are involved in temporal discounting preference (Kobayashi and Schultz, 2008; Pine et al., 2010). Furthermore, it has been reported that individuals with increased dopamine release are more inclined to choose the SSR (Joutsa et al., 2015). Crossover work in animal models might allow for direct testing of this hypothesis

(Grayson and Fair, 2017; Grayson et al., 2014; Miranda-Dominguez et al., 2014; Stafford et al., 2014).

One hypothesis is that changes in the cortico-striatal circuitry that occur in the transition into adolescence are related to hormonal changes that affect the interaction within the networks (Blakemore et al., 2010; Chambers et al., 2003). Specifically, these hormonal changes impact and influence motivation towards reward seeking behaviors (Luciana and Collins, 2012). Pubertal hormones and neurotransmitters, such as sex hormones and dopamine, affect regions across the brain, but their effects (especially dopamine) on the vmPFC, NAcc, and caudate might influence the development of cognitive capacities such as abstract thinking, problem solving, and working memory (Chambers et al., 2003).

4.3. Limitations and future directions

This study examined temporal discounting preference as it relates to biological measures. However, social environmental factors can impact an individual's subjective value of money and preference for waiting for a LLR. For example, a previous study found that individuals who grew up in lower socio-economic status environments (SES) preferred SSR, whereas individuals who grew up in higher SES environments preferred LLR (Griskevicius et al., 2013). In an experimental manipulation, Kidd et al. (2013) demonstrated that children presented with a reliable

environment demonstrated a significant increase in their delay time compared to children presented with an unstable environment. It should not be assumed that steeper discounting is always maladaptive. Very low socio-economic status populations were under-represented in the current study. Future investigations should assess how social environmental factors might impact the relationship between biological measures and temporal discounting preference.

Previous studies have shown evidence for heterogeneity in functional connectivity existing across individuals in typically developing as well as in clinical samples (Costa Dias et al., 2015; Fair et al., 2012a; Gates et al., 2014). For example, graph theory and community detection can be used to classify typically developing children into specific neuropsychological subgroups (Gates et al., 2014), and functional subgroups can be differentiated based on heterogeneity related to behavioral characteristics including impulsivity (Costa Dias et al., 2015). This study did not account for these heterogeneity present in the group and further investigation should be considerate of this phenomenon. Further, the current study utilized a brain parcellation based on anatomical boundaries (the Desikan-Killiany atlas; Desikan et al., 2006) in order to test hypotheses generated from previous work. However, establishing the consistency of these findings with other parcellations (Glasser et al., 2016; Gordon et al., 2016) will be an important next step (Grayson and Fair, 2017; Hagmann et al., 2012).

4.4. Conclusion

On average, children start to prefer waiting for later, larger rewards as they transition into adolescence. However, there is a substantial amount of variability in temporal discounting preference between individuals across development. This study provides evidence that individual differences in functional brain connectivity within and between regions in cognitive control and valuation networks can account for variance in temporal discounting preference above age. Specifically, greater connectivity strength between cognitive control regions, as well as between cognitive control and valuation regions, was related to a preference for waiting for a larger reward. In contrast, greater connectivity strength between valuation network regions was related to a preference for taking an immediate, smaller, reward. Future studies should examine the impact of social environmental factors on the relationship between functional brain connectivity and temporal discounting behavior across development.

Funding

This research was supported by R01 MH107418 (Mills, PI: Pfeifer), DeStefano Innovation Fund (Fair), R01 MH096773 (Fair), MH099064 (Nigg), MH086654 (MPI: Fair, Nigg), and MH086654 (Nigg).

Conflict of Interest

None.

Acknowledgements

We would like to thank the participants and families for their ongoing participation in this study, as well as the many staff involved in administrative tasks and data collection of this project.

Appendix A. Supplementary data

Supplementary material related to this article can be found, in the online version, at doi:<https://doi.org/10.1016/j.dcn.2018.07.003>.

References

- Achterberg, M., Peper, J.S., van Duijvenvoorde, A.C.K., Mandl, R.C.W., Crone, E.A., 2016.
- Frontostriatal white matter integrity predicts development of delay of gratification: a longitudinal study. *J. Neurosci.* 36 (6), 1954–1961. <https://doi.org/10.1523/JNEUROSCI.3459-15.2016>.
- Banich, M.T., De, La, Vega, A., Andrews-Hanna, J.R., Mackiewicz Seghete, K., Du, Y., Claus, E.D., 2013. Developmental trends and individual differences in brain systems involved in intertemporal choice during adolescence. *Psychol. Addict. Behav.: J. Soc. Psychol. Addict. Behav.* 27 (2), 416–430. <https://doi.org/10.1037/a0031991>.
- Blakemore, S.-J., Burnett, S., Dahl, R.E., 2010. The role of puberty in the developing adolescent brain. *Hum. Brain Mapp.* 31 (6), 926–933. <https://doi.org/10.1002/hbm.21052>.
- Boly, M., Phillips, C., Tshibanda, L., Vanhaudenhuyse, A., Schabus, M., Dang-Vu, T.T., et al., 2008. Intrinsic brain activity in altered states of consciousness: how conscious is the default mode of brain function? *Ann. N. Y. Acad. Sci.* 1129, 119–129. <https://doi.org/10.1196/annals.1417.015>.
- Burgess, G.C., Kandala, S., Nolan, D., Laumann, T.O., Power, J.D., Adeyemo, B., et al., 2016. Evaluation of denoising strategies to address motion-correlated artifacts in resting-state functional magnetic resonance imaging data from the human connectome project. *Brain Connect.* 6 (9), 669–680. <https://doi.org/10.1089/brain.2016.0435>.
- Callusso, C., Tosoni, A., Pezzulo, G., Spadone, S., Committeri, G., 2015. Interindividual variability in functional connectivity as long-term correlate of temporal discounting. *PLoS One* 10 (3), e0119710. <https://doi.org/10.1371/journal.pone.0119710>.
- Casey, B.J., 2015. Beyond simple models of self-control to circuit-based accounts of adolescent behavior. *Annu. Rev. Psychol.* 66, 295–319. <https://doi.org/10.1146/annurev-psych-010814-015156>.
- Chambers, R.A., Taylor, J.R., Potenza, M.N., 2003. Developmental neurocircuitry of motivation in adolescence: a critical period of addiction vulnerability. *Am. J. Psychiatry* 160 (6), 1041–1052.
- Christakou, A., Brammer, M., Rubia, K., 2011. Maturation of limbic corticostratial activation and connectivity associated with developmental changes in temporal discounting. *NeuroImage* 54 (2), 1344–1354. <https://doi.org/10.1016/j.neuroimage.2010.08.067>.
- Conners, C.K., 2003. Conners' Rating Scales: Revised Technical Manual. Retrieved from. Multi-Health Systems, New York, NY. <https://www.mhs.com/MHS-Assessment?prodname=conners3>.
- Costa Dias, T.G., Wilson, V.B., Bathula, D.R., Iyer, S.P., Mills, K.L., Thurlow, B.L., et al., 2012. Reward circuit connectivity relates to delay discounting in children with attention-deficit/hyperactivity disorder. *Eur. Neuropsychopharmacol.: J. Eur. Coll. Neuropsychopharmacol.* <https://doi.org/10.1016/j.euroneuro.2012.10.015>.
- Costa Dias, T.G., Iyer, S.P., Carpenter, S.D., Cary, R.P., Wilson, V.B., Mitchell, S.H., et al., 2015. Characterizing heterogeneity in children with and without ADHD based on reward system connectivity. *Dev. Cogn. Neurosci.* 11, 155–174. <https://doi.org/10.1016/j.dcn.2014.12.005>.
- Cross, C.P., Copping, L.T., Campbell, A., 2011. Sex differences in impulsivity: a meta-analysis. *Psychol. Bull.* 137 (1), 97–130. <https://doi.org/10.1037/a0021591>.
- Dale, A.M., Fischl, B., Sereno, M.I., 1999. Cortical surface-based analysis: I. Segmentation and surface reconstruction. *NeuroImage* 9 (2), 179–194. <https://doi.org/10.1006/nimg.1998.0395>.
- de Water, E., Cillessen, A.H.N., Scheres, A., 2014. Distinct age-related differences in temporal discounting and risk taking in adolescents and young adults. *Child Dev.* 85 (5), 1881–1897. <https://doi.org/10.1111/cdev.12245>.
- Desikan, R.S., Ségonne, F., Fischl, B., Quinn, B.T., Dickerson, B.C., Blacker, D., et al., 2006. An automated labeling system for subdividing the human cerebral cortex on MRI scans into gyral based regions of interest. *NeuroImage* 31 (3), 968–980. <https://doi.org/10.1016/j.neuroimage.2006.01.021>.
- Dosenbach, N.U.F., Koller, J.M., Earl, E.A., Miranda-Dominguez, O., Klein, R.L., Van, A.N., et al., 2017. Real-time motion analytics during brain MRI improve data quality and reduce costs. *NeuroImage* 161, 80–93. <https://doi.org/10.1016/j.neuroimage.2017.08.025>.
- Fair, D.A., Bathula, D., Nikolas, M.A., Nigg, J.T., 2012a. Distinct neuropsychological subgroups in typically developing youth inform heterogeneity in children with ADHD. *Proc. Natl. Acad. Sci. U. S. A.* 109 (17), 6769–6774. <https://doi.org/10.1073/pnas.1115365109>.
- Fair, D.A., Nigg, J.T., Iyer, S., Bathula, D., Mills, K.L., Dosenbach, N.U.F., et al., 2012b. Distinct neural signatures detected for ADHD subtypes after controlling for micro-movements in resting state functional connectivity MRI data. *Front. Syst. Neurosci.* 6, 80. <https://doi.org/10.3389/fnsys.2012.00080>.
- Fischl, B., Dale, A.M., 2000. Measuring the thickness of the human cerebral cortex from magnetic resonance images. *Proc. Natl. Acad. Sci.* 97 (20), 11050–11055. <https://doi.org/10.1073/pnas.2000033797>.
- Fischl, B., Sereno, M.I., Dale, A.M., 1999. Cortical surface-based analysis. II: inflation, flattening, and a surface-based coordinate system. *NeuroImage* 9 (2), 195–207. <https://doi.org/10.1006/nimg.1998.0396>.
- Fischl, B., Salat, D.H., Busa, E., Albert, M., Dieterich, M., Haselgrave, C., et al., 2002. Whole brain segmentation: automated labeling of neuroanatomical structures in the human brain. *Neuron* 33 (3), 341–355.
- Fischl, B., van der Kouwe, A., Destrieux, C., Halgren, E., Ségonne, F., Salat, D.H., et al., 2004. Automatically parcellating the human cerebral cortex. *Cerebral Cortex (New York, N.Y.: 1991)* 14 (1), 11–22.
- Gates, K.M., Molenaar, P.C.M., Iyer, S.P., Nigg, J.T., Fair, D.A., 2014. Organizing heterogeneous samples using community detection of GIMME-derived resting state functional networks. *PLoS One* 9 (3), e91322. <https://doi.org/10.1371/journal.pone.0091322>.
- Glasser, M.F., Sotiroopoulos, S.N., Wilson, J.A., Coalson, T.S., Fischl, B., Andersson, J.L., et al., 2013. The minimal preprocessing pipelines for the Human Connectome Project. *NeuroImage* 80 (Supplement C), 105–124. <https://doi.org/10.1016/j.neuroimage>.

- 2013.04.127.**
- Glasser, M.F., Coalson, T.S., Robinson, E.C., Hacker, C.D., Harwell, J., Yacoub, E., et al., 2016. A multi-modal parcellation of human cerebral cortex. *Nature* 536 (7615), 171–178. <https://doi.org/10.1038/nature18933>.
- Gordon, E.M., Laumann, T.O., Adeyemo, B., Huckins, J.F., Kelley, W.M., Petersen, S.E., 2016. Generation and evaluation of a cortical area parcellation from resting-state correlations. *Cerebral Cortex* (New York, N.Y.: 1991) 26 (1), 288–303. <https://doi.org/10.1093/cercor/bhu239>.
- Grayson, D.S., Fair, D.A., 2017. Development of large-scale functional networks from birth to adulthood: a guide to the neuroimaging literature. *NeuroImage* 160, 15–31. <https://doi.org/10.1016/j.neuroimage.2017.01.079>.
- Grayson, D.S., Kroenke, C.D., Neuringer, M., Fair, D.A., 2014. Dietary omega-3 fatty acids modulate large-scale systems organization in the rhesus macaque brain. *J. Neurosci.* 34 (6), 2065–2074. <https://doi.org/10.1523/JNEUROSCI.3038-13.2014>.
- Green, L., Myerson, J., McFadden, E., 1997. Rate of temporal discounting decreases with amount of reward. *Mem. Cognit.* 25 (5), 715–723. <https://doi.org/10.3758/BF03211314>.
- Greve, D.N., Fischl, B., 2009. Accurate and robust brain image alignment using boundary-based registration. *NeuroImage* 48 (1), 63–72. <https://doi.org/10.1016/j.neuroimage.2009.06.060>.
- Griskevicius, V., Ackerman, J.M., Cantú, S.M., Delton, A.W., Robertson, T.E., Simpson, J.A., et al., 2013. When the economy falters, do people spend or save? Responses to resource scarcity depend on childhood environments. *Psychol. Sci.* 24 (2), 197–205. <https://doi.org/10.1177/0956797612451471>.
- Haber, S.N., Knutson, B., 2009. The reward circuit: linking primate anatomy and human imaging. *Neuropsychopharmacology* 35 (1), 4–26. <https://doi.org/10.1038/npp.2009.129>.
- Hagmann, P., Grant, P.E., Fair, D.A., 2012. MR connectomics: a conceptual framework for studying the developing brain. *Front. Syst. Neurosci.* 6, 43. <https://doi.org/10.3389/fnsys.2012.00043>.
- Hamilton, K.R., Mitchell, M.R., Wing, V.C., Balodis, I.M., Bickel, W.K., Fillmore, M., et al., 2015. Choice impulsivity: definitions, measurement issues, and clinical implications. *Personal. Disord.* 6 (2), 182–198. <https://doi.org/10.1037/per0000099>.
- Hare, T.A., Camerer, C.F., Rangel, A., 2009. Self-control in decision-making involves modulation of the vmPFC valuation system. *Science* 324 (5927), 646–648. <https://doi.org/10.1126/science.1168450>.
- Hare, T.A., Hakimi, S., Rangel, A., 2014. Activity in dlPFC and its effective connectivity to vmPFC are associated with temporal discounting. *Front. Neurosci.* 8. <https://doi.org/10.3389/fnins.2014.00050>.
- Jenkinson, M., Beckmann, C.F., Behrens, T.E.J., Woolrich, M.W., Smith, S.M., 2012. Fsl. *NeuroImage* 62 (2), 782–790. <https://doi.org/10.1016/j.neuroimage.2011.09.015>.
- Johnson, M.W., Bickel, W.K., 2008. An algorithm for identifying nonsystematic delay-discounting data. *Exp. Clin. Psychopharmacol.* 16 (3), 264–274. <https://doi.org/10.1037/1064-1299.16.3.264>.
- Joutsa, J., Voon, V., Johansson, J., Niemelä, S., Bergman, J., Kaasinen, V., 2015. Dopaminergic function and intertemporal choice. *Transl. Psychiatry* 5, e491. <https://doi.org/10.1038/tp.2014.133>.
- Karalunas, S.L., Gustafsson, H.C., Dieckmann, N.F., Tipsord, J., Mitchell, S.H., Nigg, J.T., 2017. Heterogeneity in development of aspects of working memory predicts longitudinal attention deficit hyperactivity disorder symptom change. *J. Abnorm. Psychol.* 126 (6), 774–792. <https://doi.org/10.1037/abn0000292>.
- Kidd, C., Palmeri, H., Aslin, R.N., 2013. Rational snacking: young children's decision-making on the marshmallow task is moderated by beliefs about environmental reliability. *Cognition* 126 (1), 109–114. <https://doi.org/10.1016/j.cognition.2012.08.004>.
- Kobayashi, S., Schultz, W., 2008. Influence of reward delays on responses of dopamine neurons. *J. Neurosci.* 28 (31), 7837–7846. <https://doi.org/10.1523/JNEUROSCI.1600-08.2008>.
- Lee, N.C., de Groot, R.H.M., Boschloo, A., Dekker, S., Krabbendam, L., Jolles, J., 2013. Age and educational track influence adolescent discounting of delayed rewards. *Front. Psychol.* 4. <https://doi.org/10.3389/fpsyg.2013.00993>.
- Li, N., Ma, N., Liu, Y., He, X.-S., Sun, D.-L., Fu, X.-M., et al., 2013. Resting-state functional connectivity predicts impulsivity in economic decision-making. *J. Neurosci.* 33 (11), 4886–4895. <https://doi.org/10.1523/JNEUROSCI.1342-12.2013>.
- Luciana, M., Collins, P.F., 2012. Incentive motivation, cognitive control, and the adolescent brain: is it time for a paradigm shift? *Child Dev. Perspect.* 6 (4), 392–399. <https://doi.org/10.1111/j.1750-8606.2012.00252.x>.
- Miranda-Dominguez, O., Mills, B.D., Grayson, D., Woodall, A., Grant, K.A., Kroenke, C.D., Fair, D.A., 2014. Bridging the gap between the human and macaque connectome: a quantitative comparison of global interspecies structure-function relationships and network topology. *J. Neurosci.* 34 (16), 5552–5563. <https://doi.org/10.1523/JNEUROSCI.4229-13.2014>.
- Mitchell, S.H., Wilson, V.B., Karalunas, S.L., 2015. Comparing hyperbolic, delay-amount sensitivity and present-bias models of delay discounting. *Behav. Processes* 114, 52–62. <https://doi.org/10.1016/j.beproc.2015.03.006>.
- Myerson, J., Green, L., 1995. Discounting of delayed rewards: models of individual choice. *J. Exp. Anal. Behav.* 64 (3), 263–276. <https://doi.org/10.1901/jeab.1995.64-263>.
- Myerson, J., Green, L., Warusawitharana, M., 2001. Area under the curve as a measure of discounting. *J. Exp. Anal. Behav.* 76 (2), 235–243. <https://doi.org/10.1901/jeab.2001.76-235>.
- Odum, A.L., 2011. Delay Discounting: I'm a k, You're a k. *J. Exp. Anal. Behav.* 96 (3), 427–439. <https://doi.org/10.1901/jeab.2011.96-423>.
- Olson, E.A., Collins, P.F., Hooper, C.J., Muetzel, R., Lim, K.O., Luciana, M., 2009. White matter integrity predicts delay discounting behavior in 9- to 23-year-olds: a diffusion tensor imaging study. *J. Cogn. Neurosci.* 21 (7), 1406–1421. <https://doi.org/10.1162/jocn.2009.21107>.
- Peters, J., Büchel, C., 2010. Episodic future thinking reduces reward delay discounting through an enhancement of prefrontal-mediotemporal interactions. *Neuron* 66 (1), 138–148. <https://doi.org/10.1016/j.neuron.2010.03.026>.
- Peters, J., Büchel, C., 2011. The neural mechanisms of inter-temporal decision-making: understanding variability. *Trends Cogn. Sci. (Regul. Ed.)* 15 (5), 227–239. <https://doi.org/10.1016/j.tics.2011.03.002>.
- Pine, A., Shiner, T., Seymour, B., Dolan, R.J., 2010. Dopamine, time, and impulsivity in humans. *J. Neurosci.* 30 (26), 8888–8896. <https://doi.org/10.1523/JNEUROSCI.6028-09.2010>.
- Power, J.D., Barnes, K.A., Snyder, A.Z., Schlaggar, B.L., Petersen, S.E., 2012. Spurious but systematic correlations in functional connectivity MRI networks arise from subject motion. *NeuroImage* 59 (3), 2142–2154. <https://doi.org/10.1016/j.neuroimage.2011.10.018>.
- Power, J.D., Mitra, A., Laumann, T.O., Snyder, A.Z., Schlaggar, B.L., Petersen, S.E., 2014a. Methods to detect, characterize, and remove motion artifact in resting state fMRI. *NeuroImage* 84, 320–341. <https://doi.org/10.1016/j.neuroimage.2013.08.048>.
- Power, J.D., Schlaggar, B.L., Petersen, S.E., 2014b. Studying brain organization via spontaneous fMRI signal. *Neuron* 84 (4), 681–696. <https://doi.org/10.1016/j.neuron.2014.09.007>.
- Puig-Antich, J., Ryan, N., 1986. *Schedule for Affective Disorders and Schizophrenia for School-Age Children*. Western Psychiatric Institute and Clinic, Pittsburgh, PA.
- Richards, J.B., Zhang, L., Mitchell, S.H., de Wit, H., 1999. Delay or probability discounting in a model of impulsive behavior: effect of alcohol. *J. Exp. Anal. Behav.* 71 (2), 121–143. <https://doi.org/10.1901/jeab.1999.71-121>.
- Sadaghiani, S., Kleinschmidt, A., 2013. Functional interactions between intrinsic brain activity and behavior. *NeuroImage* 80, 379–386. <https://doi.org/10.1016/j.neuroimage.2013.04.100>.
- Scheres, A., de Water, E., Mies, G.W., 2013. The neural correlates of temporal reward discounting. *Wiley Interdiscip. Rev. Cogn. Sci.* 4 (5), 523–545. <https://doi.org/10.1002/wcs.1246>.
- Scheres, A., Tontsch, C., Thoeny, A.L., Sumiya, M., 2014. Temporal reward discounting in children, adolescents, and emerging adults during an experiential task. *Dev. Psychol.* 5, 711. <https://doi.org/10.3389/fpsyg.2014.00711>.
- Smith, S.M., Jenkinson, M., Woolrich, M.W., Beckmann, C.F., Behrens, T.E.J., Johansen-Berg, H., et al., 2004. Advances in functional and structural MR image analysis and implementation as FSL. *NeuroImage* 23 (Suppl 1), S208–219. <https://doi.org/10.1016/j.neuroimage.2004.07.051>.
- Stafford, J.M., Jarrett, B.R., Miranda-Dominguez, O., Mills, B.D., Cain, N., Mihalas, S., et al., 2014. Large-scale topology and the default mode network in the mouse connectome. *Proc. Natl. Acad. Sci. U. S. A.* 111 (52), 18745–18750. <https://doi.org/10.1073/pnas.1404346111>.
- Steinberg, L., Graham, S., O'Brien, L., Woolard, J., Cauffman, E., Banich, M., 2009. Age differences in future orientation and delay discounting. *Child Dev.* 80 (1), 28–44. <https://doi.org/10.1111/j.1467-8624.2008.01244.x>.
- van den Bos, W., McClure, S.M., 2013. Towards a general model of temporal discounting. *J. Exp. Anal. Behav.* 99 (1), 58–73. <https://doi.org/10.1002/jeab.6>.
- van den Bos, W., Rodriguez, C.A., Schweitzer, J.B., McClure, S.M., 2014. Connectivity strength of dissociable striatal tracts predict individual differences in temporal discounting. *J. Neurosci.* 34 (31), 10298–10310. <https://doi.org/10.1523/JNEUROSCI.4105-13.2014>.
- van den Bos, W., Rodriguez, C.A., Schweitzer, J.B., McClure, S.M., 2015. Adolescent impatience decreases with increased frontostriatal connectivity. *Proc. Natl. Acad. Sci.* 112 (29), E3765–E3774. <https://doi.org/10.1073/pnas.1423095112>.
- Volkow, N.D., Baler, R.D., 2015. NOW vs LATER brain circuits: implications for obesity and addiction. *Trends Neurosci.* 38 (6), 345–352. <https://doi.org/10.1016/j.tins.2015.04.002>.
- Wang, S., Zhou, M., Chen, T., Yang, X., Chen, G., Gong, Q., 2017. Delay discounting is associated with the fractional amplitude of low-frequency fluctuations and resting-state functional connectivity in late adolescence. *Sci. Rep.* 7 (1), 10276. <https://doi.org/10.1038/s41598-017-11109-z>.
- Wechsler, D., 2003. *Wechsler intelligence scale for children. (WISC-IV) Technical and Interpretive Manual*, 4th ed. Harcourt Brace, San Antonio, TX.
- Woolrich, M.W., Jbabdi, S., Patenaude, B., Chappell, M., Makni, S., Behrens, T., et al., 2009. Bayesian analysis of neuroimaging data in FSL. *NeuroImage* 45 (1 Suppl), S173–186. <https://doi.org/10.1016/j.neuroimage.2008.10.055>.
- Yi, R., Pitcock, J.A., Landes, R.D., Bickel, W.K., 2010. The short of it: abbreviating the temporal discounting procedure. *Exp. Clin. Psychopharmacol.* 18 (4), 366–374. <https://doi.org/10.1037/a0019904>.